Zurich Open Repository and Archive
University of Zurich
University Library
Strickhofstrasse 39
CH-8057 Zurich
www.zora.uzh.ch

Year: 2016

Biomechanics of the incudo-malleolar-joint - experimental investigations for quasi-static loads

Ihrle, S ; Gerig, R ; Dobrev, I ; Röösli, C ; Sim, J H ; Huber, A M ; Eiber, A

Abstract: Under large quasi-static loads, the incudo-malleolar joint (IMJ), connecting the malleus and the incus, is highly mobile. It can be classified as a mechanical filter decoupling large quasi-static motions while transferring small dynamic excitations. This is presumed to be due to the complex geometry of the joint inducing a spatial decoupling between the malleus and incus under large quasi-static loads. Spatial Laser Doppler Vibrometer (LDV) displacement measurements on isolated malleus-incus-complexes (MICs) were performed. With the malleus firmly attached to a probe holder, the incus was excited by applying quasi-static forces at different points. For each force application point the resulting displacement was measured subsequently at different points on the incus. The location of the force application point and the LDV measurement points were calculated in a post-processing step combining the position of the LDV points with geometric data of the MIC. The rigid body motion of the incus was then calculated from the multiple displacement measurements for each force application point. The contact regions of the articular surfaces for different load configurations were calculated by applying the reconstructed motion to the geometry model of the MIC and calculate the minimal distance of the articular surfaces. The reconstructed motion has a complex spatial characteristic and varies for different force application points. The motion changed with increasing load caused by the kinematic guidance of the articular surfaces of the joint. The IMJ permits a relative large rotation around the anterior-posterior axis through the joint when a force is applied at the lenticularis in lateral direction before impeding the motion. This is part of the decoupling of the malleus motion from the incus motion in case of large quasi-static loads.

DOI: https://doi.org/10.1016/j.heares.2015.10.015

Posted at the Zurich Open Repository and Archive, University of Zurich
ZORA URL: https://doi.org/10.5167/uzh-117058
Journal Article
Accepted Version

The following work is licensed under a Creative Commons: Attribution-NonCommercial-NoDerivatives 4.0 International (CC BY-NC-ND 4.0) License.

Originally published at:
Ihrle, S; Gerig, R; Dobrev, I; Röösli, C; Sim, J H; Huber, A M; Eiber, A (2016). Biomechanics of the incudo-malleolar-joint - experimental investigations for quasi-static loads. Hearing research, 340:69-78.
DOI: https://doi.org/10.1016/j.heares.2015.10.015

Accepted Manuscript

Biomechanics of the Incudo-Malleolar-Joint - Experimental Investigations for Quasi-Static Loads

S. Ihrle, R. Gerig, I. Dobrev, C. Röösli, J.H. Sim, A.M. Huber, A. Eiber

PII: S0378-5955(15)30086-1

DOI: 10.1016/j.heares.2015.10.015

Reference: HEARES 7042

To appear in: *Hearing Research*

Received Date: 31 July 2015

Revised Date: 8 October 2015

Accepted Date: 14 October 2015

Please cite this article as: Ihrle, S., Gerig, R., Dobrev, I., Röösli, C., Sim, J.H., Huber, A.M., Eiber, A., Biomechanics of the Incudo-Malleolar-Joint - Experimental Investigations for Quasi-Static Loads, *Hearing Research* (2015), doi: 10.1016/j.heares.2015.10.015.

This is a PDF file of an unedited manuscript that has been accepted for publication. As a service to our customers we are providing this early version of the manuscript. The manuscript will undergo copyediting, typesetting, and review of the resulting proof before it is published in its final form. Please note that during the production process errors may be discovered which could affect the content, and all legal disclaimers that apply to the journal pertain.

ACCEPTED MANUSCRIPT

Biomechanics of the Incudo-Malleolar-Joint
-
Experimental Investigations for Quasi-Static Loads

S. Ihrle[a,*], R. Gerig[b], I. Dobrev[b], C. Röösli[b], J.H. Sim[b], A.M. Huber[b], A. Eiber[a]

[a] *Institute of Engineering and Computational Mechanics, University of Stuttgart, Pfaffenwaldring 9, 70569 Stuttgart, Germany*
[b] *Department of Otorhinolaryngology, Head and Neck Surgery, University Hospital Zurich, Frauenkliniksrasse 24, Zurich 8091, Switzerland*

Abstract

Under large quasi-static loads, the incudo-malleolar joint (IMJ), connecting the malleus and the incus, is highly mobile. It can be classified as a mechanical filter decoupling large quasi-static motions while transferring small dynamic excitations. This is presumed to be due to the complex geometry of the joint inducing a spatial decoupling between the malleus and incus under large quasi-static loads.

Spatial Laser Doppler Vibrometer (LDV) displacement measurements on isolated malleus-incus-complexes (MICs) were performed. With the malleus firmly attached to a probe holder, the incus was excited by applying quasi-static forces at different points. For each force application point the resulting displacement was measured subsequently at different points on the incus. The location of the force application point and the LDV measurement points were calculated in a post-processing step combining the position of the LDV points with geometric data of the MIC. The rigid body motion of the incus was then calculated from the multiple displacement measurements for each force application point. The contact regions of the articular surfaces for different load configurations were calculated by applying the reconstructed motion to the geometry model of the MIC and calculate the minimal distance of the articular surfaces.

The reconstructed motion has a complex spatial characteristic and varies for different force application points. The motion changed with increasing load caused by the kinematic guidance of the articular surfaces of the joint. The IMJ permits a relative large rotation around the anterior-posterior axis through the joint when a force is applied at the lenticularis in lateral direction before impeding the motion. This is part of the decoupling of the malleus motion from the incus motion in case of large quasi-static loads.

Keywords: Incudo-malleolar joint, Malleus-incus complex, Quasi-static load, Spatial displacement, Contact, 3D-Laser-Doppler-Vibrometry, Diarthrodial joint

1. Introduction

Beside the small acoustically induced vibrations, the human middle ear has to handle large quasi-static pressure variations. Those pressure variations are several orders of magnitude larger than the acoustically induced pressure levels and are caused by ambient pressure changes as well as by every day activities like taking an elevator, flying or even changing the body posture, e.g. Hüttenbrink (1997); Dirckx (2007); Mirza and Richardson (2005).

This raises the question, how can the middle ear tolerate those massive static pressure variations while maintaining its function in case of the sound transfer? Hüttenbrink (1988) investigated the motion of the ossicular chain while applying large quasi-static pressures (± 4kPa) to the tympanic membrane. He describes flexibility within the middle ear joints protecting the inner ear by decoupling the motion of the malleus from the ossicular chain. He proposed that the complex geometric structure of the Incudo-Malleolar-Joint (IMJ) induces a change of the motion of the incus decoupling it from the stapes. Other studies have also reported a relative motion within the IMJ in case of quasi-static loads, e.g. Cancura (1980); Schön and Müller (1999).

The IMJ is known to be a true diarthrodial joint with a complex saddle shaped form of the articular faces, as described in Marquet (1981); Kirikae (1960); Etholm and Belal Jr (1974); Harty (1964); Sim and Puria (2007). Both the complex shape of the articular surface of the joint and the described spatial motion of the ossicles indicate the need of three dimensional measurements of the relative joint motion for understanding the biomechanics of the IMJ. Three dimensional investigations of the dynamic vibration of the complete ossicular chain of the middle ear with LDVs considering the geometric structure of the ossicles have been performed in the past, e.g. Decraemer et al. (1994, 2014). To our knowledge the spatial

*Corresponding author: Sebastian Ihrle
Email address: sebastian.ihrle@itm.uni-stuttgart.de (S. Ihrle)

motion of the malleus incus complex (MIC) in case of quasi-static excitation has not been investigated by spatial LDV displacement yet. Therefore we created a measurement setup capable of capturing the spatial displacement within the IMJ and correlate this motion with the geometry of the joint surface, see Ihrle et al. (2015)

The goal of this study was to investigate the mechanical behavior of the IMJ in case of quasi-static loads. To exclude the effects of other middle ear components we performed measurements on isolated MICs. We measured the spatial motion of the MIC with a 3D-LDV and reconstructed the rigid body motion. In combination with the geometry of the MIC obtained from micro-CT scans the motion was correlated with the structure of the articular surfaces of the joint.

2. Material and methods

2.1. Temporal bone preparation

Measurements were performed on five isolated MIC harvested from fresh human temporal bones (TBs) (41 - 70 years old). The temporal bones were harvested within 24 hours after death and preserved in 0.1 % thiomersal solution at 4 °C. The MIC was extracted by removing the tympanic membrane, the ligaments and the tensor tympani from the TB, and cutting the incudo-stapedial joint. The isolated MICs were checked under a microscope for damage of the joint. One MIC was excluded during the first step of measurement resulting in 4 TBs for the analysis presented in this paper.

The malleus was fixed to a probe holder with hystoacryl glue. The malleus was orientated with the axis from the umbo to the superior top of the malleus head aligned parallel to the vertical edges of the probe holder. The IMJ and the incus were able to move free and visual access was facilitated by the form of the probe holder. Foam material was placed on the block and flushed with saline solution to keep the sample moist during the measurements. Additionally, drops of saline solution were applied with a syringe to the MICs in-between the different measurements steps. Figure 1 shows the orientation of the four MICs attached to the probe holder.

2.2. Measurement system

The measurement setup and procedure are described briefly as they have been previously described in work (Ihrle et al. (2015)) related to equivalent experiments performed on artificial ossicles as a prior step to investigations on human TBs. This previous works includes descriptions of details about the measurement setup and procedure as well as the performance of the developed data- and post-processing methods has been described in detail in this previous work.

Generally, spatial Laser Doppler Vibrometer (LDV) displacement measurements were performed subsequently at several points on the incus surface with the excitation retained unchanged. The incus was excited by a stylus, while measuring the applied force and the displacement of the stylus, as shown in Fig. 2. By combining the LDV measurements from multiple points, the rigid body motion of the incus was calculated. The following procedure was repeated for each force application point: (1) A time-displacement profile of the micropositioning stage is defined; (2) The spatial displacement at different laser measurement points on the specimen surface is measured, while retaining both the time-displacement profile and the force application point unchanged. Before starting the measurement the specimen was preconditioned by applying a sinusoidal displacement profile.

2.2.1. Excitation of the malleus incus complex

In the experiments two kinds of signals were used: a low-frequency sinusoidal excitation (0.05-0.1 Hz) and a step displacement profile, both shown in Fig. 2. The sinusoidal yields the nonlinear quasi-static stiffness-values and the spatial motion of the ossicles in case of a continuous motion of the ossicles. The step displacement excitation with a holding time allows a characterization of the viscoelastic material. This was done by analyzing the relaxation curves derived from the force-time curve and by comparing the maximum and minimum force level in each load step - Silver et al. (2001).

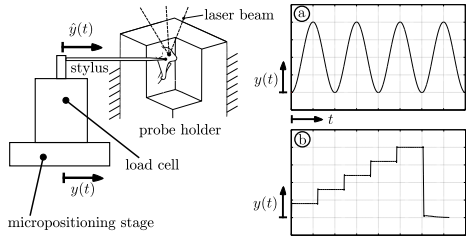

Figure 2: Schematic depiction of the excitation of the incus by a stylus. The stylus is connected to a load cell and driven by an electronic micro-positioning stage. Two kinds of excitation were used: a low frequency sinusoidal and an incremental step displacements signal. The spatial displacement of several points on the incus surface was measured by a combination of three 1D-LDVs.

For the determination of the starting point the stylus was moved forward in direction of the incus surface until a change in the force signal was measured. Then the stylus was moved slowly backwards until the force levels drops back to zero. From this position the MIC was preconditioned by applying several cycles of the sinusoidal excitation profile. After a short waiting time the procedure for the starting position determination was executed again, and after that the measurement was started. At first the sinusoidal profile was applied followed by the stepwise indentation. The application of sinusoidal and stepwise incremental displacement profiles was also used by Aernouts et al. (2012) to quantify the mechanical properties of the tympanic membrane in the quasi-static regime.

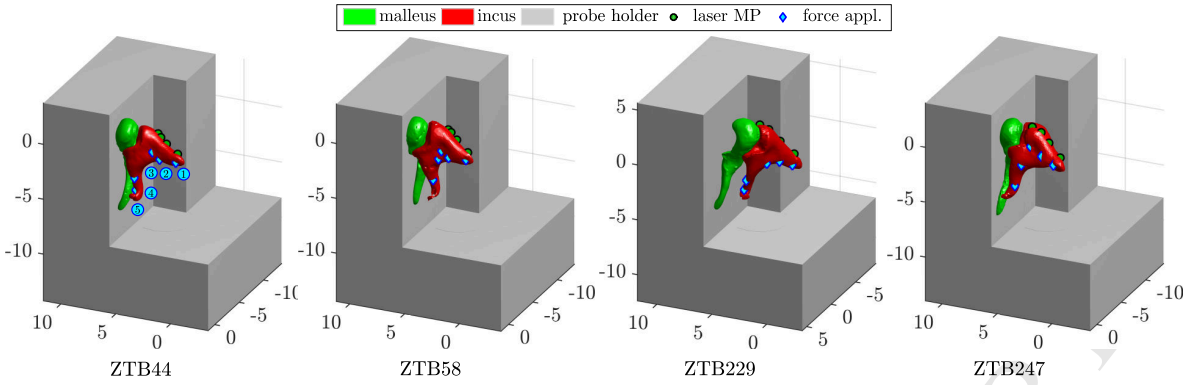

Figure 1: Orientation of the isolated malleus incus complexes (MICs) attached to the probe holder. The force application points are highlighted in blue with the numbering being consistent for all TBs. The laser measurement point are located at the superior-lateral side of the short process of incus and highlighted in green. The geometry is obtained from micro-CT scans after the measurements while the was MIC still connected to the probe holder.

We applied two ranges of displacement. In case of ZTB44/58 we applied small displacements (up to 150 μm) to focus on the ligaments and minimize the joint contact. While for ZBT229/247 the displacement range was increased (up to 400 μm) to induce joint contact and induced guidance motion of the joint surfaces.

2.2.2. *Displacement measurement*

The displacements of the points on the incus surface were measured by a combination of three linear independent aligned 1D-LDV units. The spatial displacement was calculated from the three LDV signals by transforming the data from an oblique coordinate system, spanned by the optical axes of the three LDVs to a Cartesian coordinate system. This transformation, based on matrix multiplication, is calculated in real time, allowing for intermediate availability of the spatial components during the measurement. Details about the performance and reliability of the system can be found in Ihrle et al. (2015).

For each force application point, the spatial displacement was measured at at least four non-collinear measurement points on the incus surface. Due to the complex shape of the surface of the incus, the laser beams were refocused at each new measurement point. Therefore, the mounting of the LDVs can be translated in inferior-superior-direction with a manual micrometer-driven translational stage. Each LDV-unit was equipped with a camera aligned along the optical axis of the laser beam. The position of the measurement point was monitored visually via the cameras and the location of the measurement point was quantified by the electronic positioning system of the LDV-units. Figure 3 shows the view of the video camera and the corresponding position on the MIC.

To verify the rigid connection of the malleus with the probe holder, the motion of the malleus was also measured at a point on the superior surface. For all four TBs there was no significant motion of the malleus, while a force was applied to the incus.

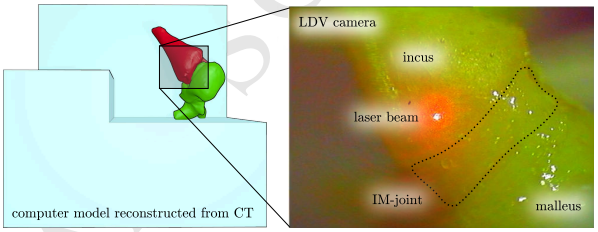

Figure 3: Parts of the MIC captured by the integrated camera of the LDV unit. The position of the LDV spot was checked visually with the position being recorded by the positioning system of the LDV unit. The coordinates of the measurement points were projected to a geometry model of the MIC derived from micro-CT scans and compared with the recorded video images.

In contrast to a 1D-LDV, the three LDV beams had to be orientated oblique to the objects surface in order to span a spatial measurement system, which minimized the amount of backscattered light. To improve the LDV signal level the surface of the incus was covered with glass beads ($\varnothing \approx 50\,\mu$m). The application of glass beads for improving the signal level has been performed by many research groups and is known to have little effect on the mechanics of the middle ear even in case of acoustic stimulation Voss et al. (2000).

Errors in the displacements signal caused by short signal loss, e.g. when one laser beam switches between glass beads, were identified and removed using a wavelet decomposition based on Haar wavelets. Details about discontinuity detection by wavelet decomposition can be found e.g. in Strang and Nguyen (1996). Figure 4 shows the 3 components of the spatial motion of a point on the superior surface of the short processus of incus of TB ZTB58.

2.3. *Micro CT imaging and frame registration*

After the spatial and force measurements, the MIC, while still connected to the probe holder, was scanned by a high-resolution micro-CT scanner (vivaCT 40, SCANCO Medical AG) with the photon energy level

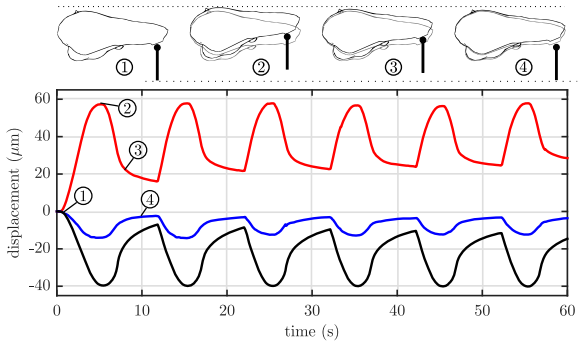

Figure 4: An example for the spatial displacement obtained for a LDV measurement point on ZTB58 by the 3D-LDV measurement system. The stylus was displaced by applying a low frequency (0.1 Hz) sinusoidal excitation signal. The varying load induces a complex spatial motion with significant components in all three spatial directions is monitored. At the first loading cycle, when the stylus is moved back to zero position, it loses contact (at time marked by 3) with the sample due to the high viscoelastic behavior of the IMJ, which causes a residual non-zero minimal displacement, which reaches a constant value in the subsequent loading cycles.

set to 55 keV, see Sim and Puria (2007). The probe holder was highlighted with a metallic marker (Edding 780 Glanzlack, Wunstdorf, Germany) and additional copper wires were glued to the probe holder to provide more robust determination of its orientation. Both the metal marker and the copper wires were clearly visible in the CT-image due to their high x-ray attenuation.

To reconstruct the spatial motion of the MIC, surface models of the incus, the malleus and the probe holder were obtained from the CT data. The surface models were imported to open source 3D software (Blender 2.72), where they were aligned with the probe holder orientated according to the measurement system, defined in Fig. 1 and exported in the STL data format for further post-processing.

2.4. Reconstruction of the spatial motion

The position and orientation of a rigid body can be described using the set of generalized coordinates

$$\mathbf{q}^I(t) = \begin{bmatrix} u_x(t) & u_y(t) & u_z(t) & \alpha(t) & \beta(t) & \gamma(t) \end{bmatrix}^{\mathrm{T}}. \quad (1)$$

The spatial displacements $\mathbf{u}_i^I(t)$ measured by the 3D-LDV at $n \geq 3$ non-collinear points P_i are combined to form the overdetermined system of equations

$$\begin{bmatrix} \mathbf{u}_1^I(t) \\ \vdots \\ \mathbf{u}_n^I(t) \end{bmatrix} = \begin{bmatrix} \mathbf{A}_1 \\ \vdots \\ \mathbf{A}_n \end{bmatrix} \mathbf{q}^I(t). \quad (2)$$

The generalized coordinates $\mathbf{q}^I(t)$ of the incus are calculated by solving Eq. (2) with the method of minimizing the least square error. The submatrix

$$\mathbf{A}_i = \begin{bmatrix} 1 & 0 & 0 & 0 & a_{i,z}^I & -a_{i,y}^I \\ 0 & 1 & 0 & -a_{i,z}^I & 0 & a_{i,x}^I \\ 0 & 0 & 1 & a_{i,y}^I & -a_{i,x}^I & 0 \end{bmatrix} \quad (3)$$

contains the coordinates $\mathbf{a}_i^I$ of the measurement point P_i.

The positioning of the laser beams on the specimen was done my moving the specimen, with the LDV beams pointing on a fixed point in space and the focus adjusted at the beginning of the measurement. When the incus was moving, the LDVs were still focused on the same point in space, which means that the position of the measurement points on the incus was changing. In case of small dynamic excitations, the effects of these variations can be neglected, but for the investigated displacements they have to be taken into account. Therefore, the positions of the measurement point were updated for each time step as follows: (1) The orientation and location of the surface model of the incus was updated based on the previous time step; (2) The intersection between virtual laser beams fixed in space and located at the initial measurement positions and the surface model were calculated using a custom raytracing algorithm; (3) The coordinates of the measurement points in Eq. (2) were updated and the generalized coordinates of the current time step were calculated by solving Eq. (2). The raytracer was implemented in Matlab and based on the OPCODE collision detection library by Terdiman (2001).

2.5. Determination of the contact area

The contact of the two articular surfaces of the IMJ during the excitation could be identified with the position and orientation of the incus. At each time step, with the updated position and orientation of the incus, the distances between the two articular surfaces were calculated along the surface area with the vtkDistancePolyDataFilter of the Visualization Toolkit (VTK), an open source software library for 3D computations. For the analysis of the complete dataset of an excitation position, i.e. the updated geometry and distance values for every time-step, was imported into Paraview, an open source post-processing software. In Paraview, different characteristic values, e.g. min/max, standard-deviation, etc. were calculated.

3. Results

3.1. Force-displacement curves

The force-displacement curves derived from the load cell and the displacement of the stylus for the excitation in lateral direction are shown in Fig. 6 for TBs ZTB44/58 and in Fig. 5 for TBs ZTB229/247. The force-displacement curves show a prominent hysteresis loop. The area enclosed by the load displacement curves corresponds to the energy dissipated in a cycle. When the load is applied at extremal positions (further from the IMJ) of the incus, the motion is dominated by rotational components and the relative enclosed area increases.

ACCEPTED MANUSCRIPT

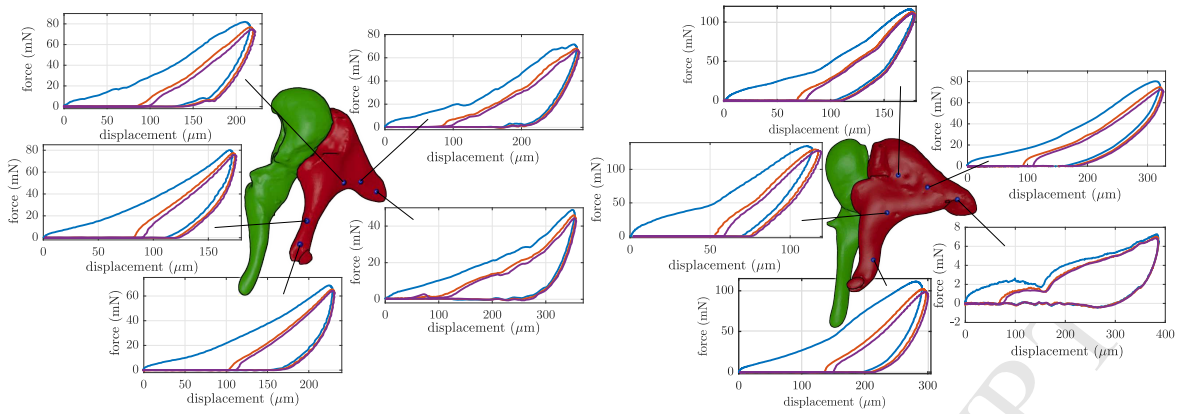

Figure 5: Summary of the force-displacement curves obtained for the excitation of the incus of TBs ZTB229/247 in lateral direction. The first loop differs from the following loops due to the different loading configuration caused by loosening of the contact between the stylus and the incus when the stylus is driven away from the incus. The displacement was chosen larger for these two TBs to induce contact between the joint surfaces. Contrary to the prior TBs the loading path cannot be described by a linear approximation. The slope varies with the force application location, with most prominent changes at the area near the articular surfaces. The force-displacement curves at force application point 1 of ZTB247 show very small forces caused by slippage of the stylus and are neglected in the data processing.

The first hysteresis loop shows a significant difference to the following ones, caused by a different loading path. Even in case of this very low frequency excitation the incus has not returned to its initial position at the end of the first loop. When the stylus is moved again in the lateral direction, it touches the incus surface at a moment when the incus is still in a still deflected position, as evidenced by Fig. 4. The following hysteresis loops are similar to each other indicating that the motion of the IMJ has reached a steady state.

The loading paths of the TBs ZTB44/58 can be described by a linear approximation, i.e. by a uniform stiffness value for each force application point, respectively. The displacement amplitudes were chosen small, with the ligaments dominating the characteristic of the joint. As the displacement amplitude was increased, as in case of the TBs ZTB229/247, the shape of the force-displacement curves became more complex. The slope of the loading path varied with the force application position, with most prominent changes at the area near the articular surfaces.

3.2. *Viscoelasticity - step excitation*

To investigate the viscoelasticity of the IMJ stepwise displacement profiles with a holding time were applied. Figure 7 illustrates the time series of the displacement of the stylus, the applied force and the three dimensional motion of a point on the surface of the incus, when a force was applied at point Nr. 3 of TB ZTB247. The rise time of the displacement signal is 70 μs and the holding time is 12 s with a minimal increase during the holding time, caused by the motion of the incus. The force signal decreases with time which is typical for viscoelastic materials. The decrease can be approximated by two exponential functions, i.e. two time constants, describing an initial rapid decay followed by a slow decrease of the signal. The spatial

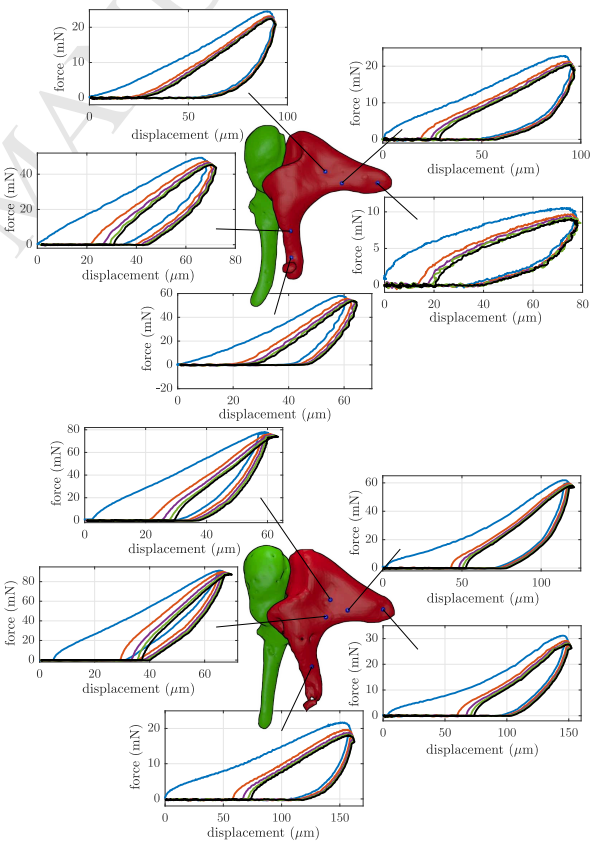

Figure 6: Summary of the force-displacement curves obtained for the excitation of the incus of TBs ZTB44/58 in lateral direction. The first loop differs from the following loops due to the different loading configuration caused by loosening of the contact between the stylus and the incus when the stylus is driven away from the incus. The displacement was chosen small for these two TBs to prevent contact between the joint surfaces. The loading paths of the TBs ZTB44/58 can be described accurately by a linear approximation, i.e. by a uniform stiffness value for each force application point, respectively.

displacement obtained from the 3D-LDV shows components in all three directions, the most prominent motion is in direction of the excitation. The motion in inferior-superior direction changes as the displacement is increased. When the incus is unloaded in the last step, it slowly returns to its initial configuration, dampened by the viscous component of the ligaments of the joint capsule.

3.3. Connection between the force-displacement curves and the joint geometry

Figure 8 shows the force-displacement curves derived from the incremental (left) and the sinusoidal (middle) displacement signal and the reconstructed spatial motion of the incus (right) in case of a sinusoidal excitation of TB ZTB247 at application point 3.

In case of the incremental displacement signal two different curves are shown. The upper curve shows the force-displacement curve calculated from the force and displacement values directly after the displacement increment. The lower curve is derived from the force and displacement value at the end of each incremental step indicating progressive behavior with a continuous increase in slope. The upper curve shows a variation of the slope with the same characteristic as the loading path of the corresponding sinusoidal curve. To identify the source of these variations, their positions are marked in both curves and compared with the reconstructed motion at the equivalent time step. The comparison indicates a connection between the change of the slope and the change of the motion of the incus. The connection between the change of the motion and the change of the slope in the force-displacement curve was found for several force application points of ZTB229/247, whereas the intensity of the changes in the spatial curve correspond to those in the force-displacement curves.

3.4. Contact areas of the articular surfaces

To explain the source for the change in the spatial motion of the incus, we determined the areas of contact of the IMJ by calculating the distance of the articular surfaces. Figure 9 and 10 illustrate the time series of the articular distance and the corresponding motion of the incus for the application point 3 and 5 of ZTB247, respectively. The motion was amplified by a factor of three for better visualization and it is drawn at different time steps corresponding to the individual IMJ distance maps on the left of Figs 9 and 10.

The distance of the articular surfaces in the unloaded state varies in the range of 25 to 280 μm, with a narrow gap on the inferior lateral and inferior medial side of the joint. Depending on the force application point, different regions of the articular surfaces come into close proximity or in contact.

In case of the application point five located near the long process of the incus, the spatial motion is dominated by a rotational component. As the load is increased the ossicles come close in proximity in the superior region of the articular faces. The rotational motion around the anterior-posterior axes is not impeded by the articular surfaces, but it is slightly guided in the superior direction as indicated by the trajectories.

4. Discussion

4.1. Measurement procedure

The goal of this study was to investigate the mechanical behavior of the IMJ in the case of quasi-static loads. To exclude the effects of other middle ear components, we performed measurements on isolated MICs. , In the literature several investigations have been performed on intact middle ear structures. In Decraemer et al. (2008) and Buytaert et al. (2013) the spatial motion of the ossicles in case of quasi-static pressure application was derived from CT scans. These investigations help to investigate if there is a spatial motion within the ossicles and if the IMJ is flexible in case of quasi-static excitation. However, from these measurements it is difficult to derive a mechanical model of the IMJ, describing the physical mechanism behind the measured phenomena and identify the corresponding model parameters. Another important factor is, that by using CT-scan information for the reconstruction of the motion, the loading path, i.e. the actual motion of the ossicles cannot be captured.

In Dirckx et al. (2005) the continuous motion including the viscoelastic effects is captured by measuring the displacement using 1D-LDV. With these investigations the existence of velocity related damping mechanism in case of quasi-static low frequency excitation can be detected. Due to the lack of spatial measurements of the motion the actual motion of the ossicles and therefore the motion within the joints cannot be determined. Therefore, it is possible to show that damping effects are present but it is very difficult to describe their cause.

The most detailed work on the quasi-static behavior of the middle ear ossicles was performed by Hüttenbrink (1988) where the spatial displacement of the ossicles was measured visually under a surgical microscope. Hüttenbrink (1988) proposed the importance of the articular surface of the IMJ for the protection of the inner ear since they induce a decoupling motion in case of large quasi-static pressure variations.

By combining spatial displacement measurements, the application of specific loads at different location, and the reconstruction of the geometry of the IMJ we can investigate the mechanical mechanism of the IMJ. In our measurements the relative motion between the articular surfaces is smaller than the values given by Hüttenbrink (1988) when we compare the joint motion induced by the lateral-medial displacement values given for the umbo motion with the joint motion caused by the largest motions of the lenticularis of the incus. He described a mean umbo displacement of -400 μm for a negative pressure of 4kPa in the ear chan-

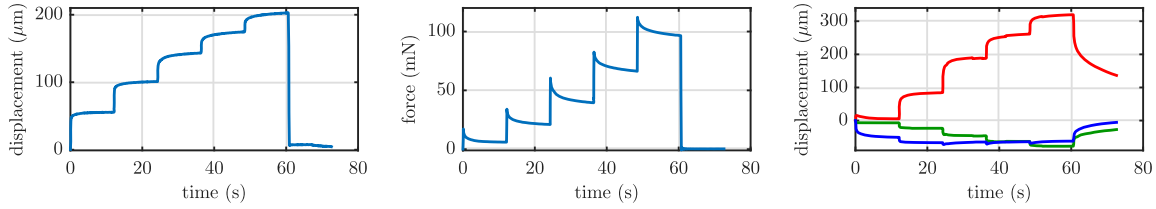

Figure 7: An example of the time series of the displacement and the force applied by the stylus at the force application point 3 of ZTB247, driven by an incremental signal. The force signal decreases with time during the holding time which is typical for viscoelastic materials. The plot on the right hand side shows the corresponding spatial displacement obtained from the 3D-LDV system. While all three components of motion indicate displacements, the most prominent motion is in the direction of the excitation (red). The motion in inferior-superior direction (blue) changes as the displacement is increased. When the incus is unloaded in the last step, it slowly returns to its initial configuration, dampened by the viscous component of the ligaments of the joint capsule.

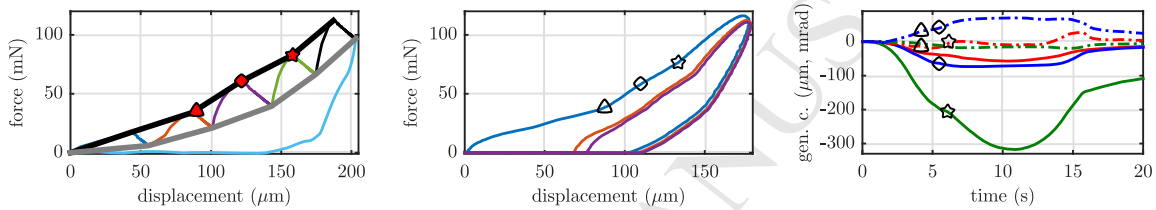

Figure 8: A comparison of the force-displacement curves of the incremental displacement excitation (left) with those in case of the low frequency sinusoidal excitation (middle) for a force application at point 3 of ZTB247. The lower curve, in case of the incremental displacement is derived from the force and displacement values at the end of each incremental step and has a progressive behavior with a continuously increasing slope. The upper curve shows a variation of the slope with the similar characteristics as the loading path of the corresponding sinusoidal curve. The plot on the right side shows the reconstructed spatial motion of the incus for the first excitation loop of the sinusoidal excitation. The curves describe the generalized coordinates of the incus, i.e. the translation and rotational rigid body motion. To identify the source of these variations, their positions are marked in both curves and compared with the reconstructed motion at the equivalent time step.

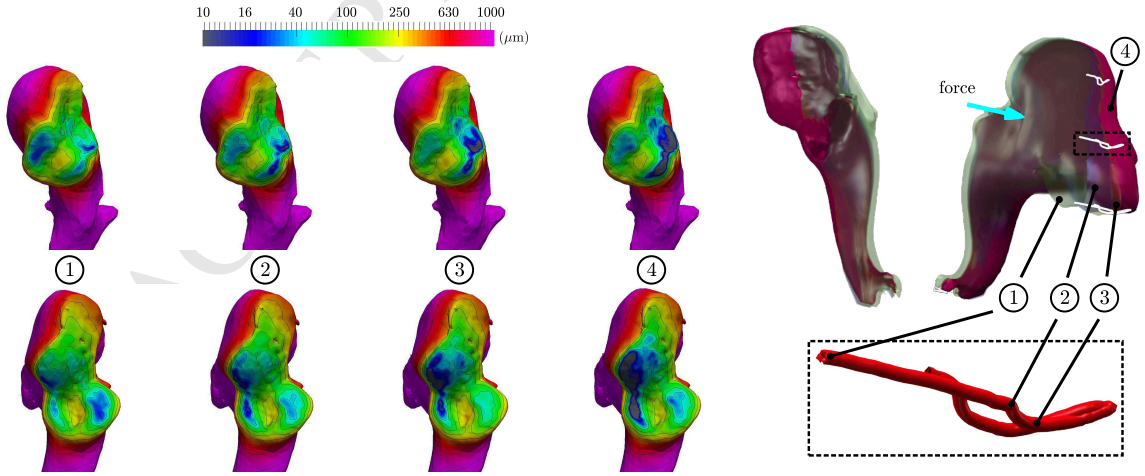

Figure 9: A visualization of the shortest distance of the joint surfaces at different time steps of the loading path, when a force is applied at application point 3 of ZTB247. As the loading of the incus is increased the medial surface of the joint gets into contact impeding the motion of the incus. On the right hand side the motion of the incus is visualized at the corresponding time steps. For better visualization the motion was magnified by a factor of three. The trajectories of the motion of points on the superior surface of the incus, indicate a prominent change of the direction of the motion during the loading path.

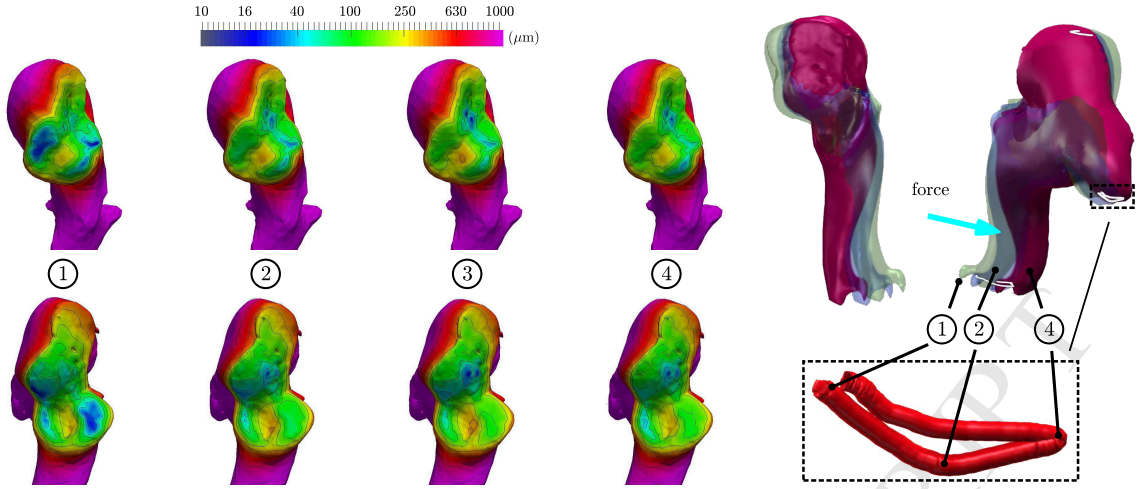

Figure 10: Applying the same visualization as described in Fig. 9 with a force applied at application point 5 of ZTB247. The spatial motion is dominated by a rotational motion around the anterior-posterior axis through the joint. This motion is not impeded by the articular surfaces, but it is slightly guided in superior direction as visualized by the motion trajectories.

nel and a mean value of 200 μm for a positive ear canal pressure of 4kPa.

The investigations were performed on isolated ossicles with the malleus being fixed. Additionally, the middle ear ligaments and tendons as well a the tympanic membrane have been removed. By performing measurements on the isolated ossicles the effects of middle ear structures beside the IMJ on the motion of the MIC can be excluded. Therefore, the question may arise if the results are still relevant, since they where deduced from a nonphysical configuration. The aim of this paper is the investigation of the biomechanics of the IM-joint. To understand the underlying mechanical mechanism, the application of different loadings, including unphysiologic configurations, is necessary to identify the load dependent behavior of different components of the IMJ, for example the articular surfaces and the ligaments of the joint capsule. With the mechanical mechanism identified, the behavior of the IMJ can be described for a broad range of different loading configurations including physiological configurations and unphysiological loading as occurring in middle ear surgery. The motion of the MIC, with the malleus being fixed at the probe holder, differs from the physiological motion in case of quasi-static pressure loads of the tympanic membrane. With the middle ear ligaments being intact, the MIC would perform a rotational motion around the anterior-posterior axis. However, the characteristic of the IM-joint is determined by the relative motion within the joint. The application of point loads on the incus, with the malleus being fixed, caused relative motions within the joint which were comparable to the motion described in the literature, e.g. Hüttenbrink (1988); Murakami et al. (1997). To compare the motion with the values given in the literature the motion of distinct points on the ossicles, e.g. umbo and lenticularis, can be derived from the reconstructed rigid body motion. Therefore even in unpysiological configurations of the middle ear, the relative motions within the IM-joint are in a physiological range when applying the presented displacement profiles at defined points on the incus.

The performance of the measurement system and the post-processing procedure have been checked in a prior investigation on artificial ossicles, see Ihrle et al. (2015). When performing measurements on irregular geometrical structures, the determination of the relative orientation between the specimen and the measurement system is crucial. This also applies to the spatial location of the measaurement points. By connecting the ossicles to a well-defined probe holder, the orientation can be identified very accurate. The exact location of the measurement point is calculated by raytracing, with the location of the point being updated during the measurement. This procedure drastically improves the quality of the reconstructed motion in case of large quasi-static motions. The complexity of the measurement setup increases tremendous when performing spatial 3D measurements instead of 1D measurements while the signal level and visual access decrease due to the oblique orientation of the three independent laser beams. Therefore, previous investigations on a reference model are inevitable for the optimization of both, the measurement setup and the post-processing procedure.

4.2. Viscoelastic properties of the IMJ

Incremental load steps were applied to the incus to quantify the viscous and the elastic response of the IMJ. Hereby, the elastic response is derived from the force-displacement relation at the end of each load step. While this method is often used to characterize the mechanical properties of soft tissue, e.g. Silver (2006), our data of the IMJ indicates qualitative difference in the shape of the derived curves, shown in Fig. 8. Due to the viscous component of the liga-

ments of the joint capsule, the relative motion of the articular surfaces differs at the beginning and at end of the load step, causing differences in the shapes of the two force-displacement curves. The force induced by the incremental elongation of the ligaments of the joint capsule decreases causing an additional relative motion along the articular surfaces. In case of the low-frequency sinusoidal excitation the articular surface of the incus is moved continuously along the counterpart of the malleus resulting in a similar shape of the force-displacement curve. This indicates that the relative motion in the IMJ is strongly influenced by the time history of the previous motion of the ossicles. This is caused by a complex interaction between the viscoelastic properties of the ligaments of the IMJ and the motion guidance of the articular faces.

To estimate the influence of the ligaments on the damping of the joint we calculated the distance between the ligaments attachment points on the rim of the joint surface for the loaded and unloaded condition. The elongation of the ligaments is strongly correlated with the size of the hysteresis of the force-displacement curve indicating that the ligaments are the main source of dissipation. This is in agreement with the report of very low friction coefficients in diarthrodial joints, e.g. in Mow et al. (1990).

4.3. The IMJ as a mechanical filter

The IMJ can be classified as a mechanical filter which decouples large quasi-static variations, e.g. caused by ambient pressure variations, and conducts small dynamic vibrations induced by acoustical excitation. The cause behind this filter is the mechanics of the connection of the malleus and the incus by a diarthrodial joint encapsuled by a highly viscoelastic ligaments. Before analyzing the function of the IMJ for the case of quasi-static excitation we will review some of the important structures of diarthrodial joints.

4.3.1. Diathroidal joints

The IMJ is a diarthrodial joint with a saddle shaped articular surface covered with synovial fluid encapsuled by fibrous joint capsule, e.g. Marquet (1981); Etholm and Belal Jr (1974) and Harty (1964).

In Mow and Huiskes (2005) diarthrodial joints are generally described as a combination of synovial fluid, articular cartilage and supporting bone that provide a smooth, nearly frictionless bearing system of the mammalian body. The ligaments provide stability to maintain the proper position of the bones. Generally diarthrodial joints are assumed to function at very low operating speeds permitting a large relative motion between opposite bones.

Those characteristics of diarthrodial joints meet exactly the requirements of the ossicular chain in case of large quasi-static variations. They permit the large motion at very low operating speeds, e.g. in case of pressure variations. The transfer of the small dynamic vibrations is done by the highly viscoelastic ligaments transferring those vibrations from the malleus to the incus.

The spatial motion between the malleus and incus in case of large quasi-static excitations is mainly determined by the saddle shaped surface of the joint. In the unloaded state the distance between the articular surfaces for all four TBs was within the range of 25 to 280 μm which is comparable to recent investigations of De Greef et al. (2015).

Dirckx et al. (2005) proposed that friction effects are important in the quasi-static regime, but viscoelasticity may be the remaining factor at acoustic frequencies. The importance of friction was motivated by the increase of hysteresis with decreasing variation rates. Although friction may contribute to the hysteresis, it is more likely, that the different loading path has a larger effect. The friction in between diarthrodial joints is generally very low, with the synovial fluid reducing the friction by lubrication of the joint surfaces and providing nutrition of the articular cartilage, Nigg and Herzog (1999); Mow et al. (1990).

4.3.2. The function of the IMJ in case of quasi-static excitations

The saddle shaped articular surfaces of the IMJ cause a decoupling motion between the malleus and incus for large quasi-static loads. This change in the motion was present at all force application points of ZTB229/247 and was correlated with variation in the force-displacement curves caused by contact of the joint surfaces. The relative rotation around the anterior-posterior axis through the joint caused only small contact of joint surfaces, with a guidance motion in inferior superior direction. The IMJ permits a relative large rotational motion before impeding such a motion, resulting in a decoupling between the malleus and incus at quasi-static loading conditions. This is in agreement with the investigations of Hüttenbrink (1988), which concerned quasi-static pressure loading of the tympanic membrane. He describes a rotational motion of the malleus with the umbo moving in lateral-medial direction and a very small motion of the lenticularis which is orientated in superior-inferior direction. He also described a guidance motion of the incus in this direction caused by the articular surfaces and stabilized by the fish-tailed posterior ligament of the incus. Although we investigated isolated MICs, the inferior-superior guidance motion caused by the contact of the superior part of the joint surfaces was also visible in our experiments. This is due to the physiological nature of the relative motion around the anterior-posterior axis between the malleus and incus.

The characteristic of the mechanical filter depends on the relative motion within the joint. Therefore, even with the malleus fixed, a physiological relative motion can be induced by applying a force at the incus.

A force, applied at the long process of incus caused a relative motion within the joint which was mainly determined by the rotational motion around the anterior-

posterior axis. This motion is in good agreement with the motion described in physiological configurations. Hence, it is not surprising, that the superior-inferior guidance motion of the joint is present in our investigations and in the motions in case of physiological pressure loads described by Hüttenbrink (1988).

A force, applied at the short processus of incus caused a rotation around the superior inferior axis with large contact area of the joint surface. Although this motion is not described in literature, due to its non-physiologic nature, it could be relevant in case of reconstructed middle ear, when a preload is applied at the ossicular chain. Additionally, the force and displacement values are within the ranges given by Lauxmann et al. (2012) for the application of different kinds of stapes prosthesis. The manipulations performed by the surgeon are comparable to the application of point loads at different locations of the incus. Hence, the presented results are also relevant for clinical applications and will improve the numerical investigation of surgical manipulation by computational models.

Based on his anatomic investigations Marquet (1981) deduced that the full joint activity includes a flexion of 500 μm of the long process of incus on the handle of the malleus. This is in agreement with our finding of a relatively large rotational motion of the incus around the anterior-posterior axis, before inducing a contact of the articular surfaces that impedes the motion. Marquet (1981) also described that the malleal

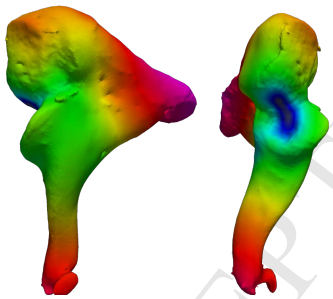

Figure 11: Visualization of the standard deviation of the spatial norm of the displacement at the maximum force level of ZTB247. Regions with a low value are highlighted in dark gray/blue, larger values are colored in red. The short and long processus of incus show large values, since their motion is very different for a force applied near the short processus and the lenticulars, see Fig. 9 and 10. The ball socket region of the incus shows a low deviation of the indicating a comparable motion in this region for all force application points.

ball is the true center of rotation of the joint. Figure 11 shows the standard deviation of the magnitude of the maximal displacement for ZTB247 for the five force application points. The region with small deviation coincidences with the ball socket region supporting a rotational motion around this region for different force application points.

For small motion of the incus, as investigated in case of ZTB44/58, the influence of the joint surface on the relative motion was small, with a linear relationship between the applied force and displacement. This is agreement with the investigations of Schön and Müller (1999) where small forces were applied at the long processus of incus, while keeping the malleus and tympanic membrane fixed, analogous to our measurement setup.

4.3.3. Consequences for the sound transfer

The studies of Nakajima et al. (2005) and Willi et al. (2002) found that in the case of acoustic excitation, the IMJ is mobile. In our recent study Gerig et al. (2015) we investigated the influence of a fixation of the IMJ on the sound transfer by measuring the stapes motion and found an increase in the middle ear transfer function above 2 kHz.

The investigations of the dynamic transfer of the IMJ show, that the IMJ balances flexibility necessary for handling quasi-static loads against a sound transfer function under acoustical excitation.

4.3.4. Consequences for the modeling of the IMJ

Mathematical modeling of the IMJ behavior under quasi-static excitation requires adequate modeling of the mechanics of the diarthrodial joint. Therefore, the geometry of the articular surfaces, the ligaments, as well as their viscoelastic properties has to be included in the model. We will include a detailed mathematical model of the IMJ in our existing elastic multibody system of the human middle ear presented in Ihrle et al. (2012). The contact of the articular surfaces will be implemented using a penalty based contact formulation utilizing the geometric information obtained from the micro-CT scans. The ligaments of the joint capsule will be modeled by distributing standard-linear-solid elements along the joint capsule, with the position and orientation being derived from the micro-CT scans. The ligaments of the joint capsule are preloaded to maintain the proper position of the ossicles. Therefore load dependent stiffness parameters will be used for the standard-linear-solid elements. The parameter values will be obtained by minimizing the spatial distance as well as the resulting force between the simulation and the measurement and will be presented in the future.

5. Conclusion

Measurements on isolated MICs were performed by applying quasi-static loads at different locations of the incus with the malleus rigidly connected to a probe holder. The spatial motion of the incus was reconstructed by performing spatial displacement measurements with a 3D-LDV on several points on the incus surface. The geometry of the MICs was derived from micro-CT scans performed after the measurement. The contact regions of the articular surfaces for different load configurations were quantified by applying the reconstructed motion to the geometry model of the MIC and calculating the minimal distance of the articular surfaces.

The reconstructed motion showed a change in the motion direction caused by the contact between the articular surfaces of the IMJ. The force-displacement curves showed a variation of the slope correlated with the guidance motion of the joint surfaces. The IMJ permits a relative large rotation around the anterior-posterior axis through the joint, when a force is applied at the lenticularis in lateral direction, before impeding the motion. This is part of the decoupling mechanism of the malleus motion from the incus motion, under large quasi-static loads. The IMJ can be classified as a mechanical filter which decouples large quasi-static variations, e.g. caused by ambient pressure variations, while transferring small dynamic vibrations induced by acoustical excitation. The mechanical mechanism behind this filter is related to the connection of the malleus and the incus by a diarthrodial joint encapsuled by a highly viscoelastic ligaments.

In future work we will extend our simulation model of the human middle ear, presented in Ihrle et al. (2012) by a detailed mathematical model of the IMJ including the geometry and the contact of the articular surfaces.

Acknowledgements

This work has been partially supported by the German Research Foundation (DFG) within the Ei 231/6-1 Grant and by the SNF (Swiss National Foundation) within the project no. 138726. This support is gratefully acknowledged.

References

Aernouts, J., Aerts, J.R., Dirckx, J.J., 2012. Mechanical properties of human tympanic membrane in the quasi-static regime from in situ point indentation measurements. Hearing Research 290, 45–54.

Buytaert, J., Aerts, J., Salih, W., De Greef, D., Peacock, J., Dierick, M., Van Hoorebeke, L., Dirckx, J., 2013. Visualizing middle ear structures with ct–studying morphology (bone and soft tissue) & dynamics, in: 1st International Conference on Tomography of Materials and Structures (ICTMS).

Cancura, W., 1980. On the statics of malleus and incus and on the function of the malleus-incus joint. Acta Oto-laryngologica 89, 342–344.

De Greef, D., Buytaert, J.A., Aerts, J.R., Van Hoorebeke, L., Dierick, M., Dirckx, J., 2015. Details of human middle ear morphology based on micro-ct imaging of phosphotungstic acid stained samples. Journal of Morphology 276, 1025–1046.

Decraemer, W., de La Rochefoucauld, O., Funnell, W., Olson, E., 2014. Three-dimensional vibration of the malleus and incus in the living gerbil. Journal of the Association for Research in Otolaryngology 15, 483–510.

Decraemer, W.F., Gea, S.L., Maas, S.A., Dirckx, J.J.J., 2008. A method for three-dimensional displacement and deformation measurement applied to the statically loaded middle ear ossicles, pp. 70980B–70980B–13.

Decraemer, W.F., Khanna, S.M., Funnell, W.R.J., 1994. A method for determining three-dimensional vibration in the ear. Hearing Research 77, 19–37.

Dirckx, J.J.J., 2007. Middle ear static pressure: Measurement, regulation and effects on middle ear mechanics, pp. 17–27.

Dirckx, J.J.J., Buytaert, J.A.N., Decraemer, W.F., 2005. Quasi-static transfer function of the rabbit middle ear, measured with a heterodyne interferometer with high-resolution position decoder. Jaro 7, 339–351.

Etholm, B., Belal Jr, A., 1974. Senile changes in the middle ear joints. The Annals of otology, rhinology, and laryngology 83, 49.

Gerig, R., Ihrle, S., Röösli, C., Dalbert, A., Dobrev, I., Pfiffner, F., Eiber, A., Huber, A.M., Sim, J.H., 2015. Contribution of the incudo-malleolar joint to middle-ear sound transmission. Hearing Research 327, 218 – 226.

Harty, M., 1964. The joints of the middle ear. Zeitschrift für mikroskopisch-anatomische Forschung 71, 24.

Hüttenbrink, K.B., 1988. The mechanics of the middle-ear at static air pressures: The role of the ossicular joints, the function of the middle-ear muscles and the behaviour of stapedial prostheses. Acta Oto-Laryngologica. Supplementum 451, 1–35.

Hüttenbrink, K.B., 1997. The middle ear as pressure receptor, in: Huettenbrink, K.B. (Ed.), Proceedings of the 1st Symposium on Middle Ear Mechanics in Research and Otology.

Ihrle, S., Eiber, A., Eberhard, P., 2015. Experimental investigation of the three dimensional vibration of a small lightweight object. Journal of Sound and Vibration 334, 108 – 119.

Ihrle, S., Lauxmann, M., Eiber, A., Eberhard, P., 2012. Nonlinear modelling of the middle ear as an elastic multibody system-applying model order reduction to acousto-structural coupled systems. Journal of Computational and Applied Mathematics 246, 18–26.

Kirikae, J., 1960. The Middle Ear. University of Tokyo Press, Tokyo.

Lauxmann, M., Heckeler, C., Beutner, D., Lüers, J.C., Hüttenbrink, K.B., Chatzimichailis, M., Huber, A., Eiber, A., 2012. Experimental study on admissible forces at the incudo-malleolar joint. Otology & Neurotology 33, 1077–1084.

Marquet, J., 1981. The incudo-malleal joint. Journal of Laryngology and Otology 95, 543–565.

Mirza, S., Richardson, H., 2005. Otic barotrauma from air travel. Journal of Laryngology & Otology 119, 366–370.

Mow, V.C., Huiskes, R. (Eds.), 2005. Basic Orthopaedic Biomechanics & Mechano-Biology. Lippincott Williams & Wilkins, Philadelphia. 3 edition.

Mow, V.C., Ratcliffe, A., Woo, S.L.Y. (Eds.), 1990. Biomechanics of Diarthrodial Joints. volume 2. Springer, New York.

Murakami, S., Gyo, K., Goode, R.L., 1997. Effect of middle ear pressure change on middle ear mechanics. Acta Otolaryngol. 117, 390–395.

Nakajima, H.H., Ravicz, M.E., Merchant, S.N., Peake, W.T., Rosowski, J.J., 2005. Experimental ossicular fixations and the middle ear's response to sound: Evidence for a flexible ossicular chain. Hearing Research 204, 60 – 77.

Nigg, B.M., Herzog, W., 1999. Biomechanics of the Musculo-Skeletal System. Wiley, Chichester. 2 edition.

Schön, F., Müller, J., 1999. Measurements of ossicular vibrations in the middle ear. Audiology and Neurotology 4, 142–149.

Silver, F.H., 2006. Mechanosensing and Mechanochemical Transduction in Extracellular Matrix: Biological, Chemical, Engineering, and Physiological Aspects. Springer, Berlin.

Silver, F.H., Bradica, G., Tria, A., 2001. Viscoelastic behavior of osteoarthritic cartilage. Connective tissue research 42, 223–233.

Sim, J.H., Puria, S., 2007. Soft tissue morphometry of the malleus incus complex from micro-ct imaging. Journal of the Acoustical Society in America 9, 5–21.

Strang, G., Nguyen, T., 1996. Wavelets and Filter Banks. Wellesley-Cambridge Press, Wellesley. 2nd edition.

Terdiman, P., 2001. Memory-optimized bounding-volume hierarchies.

Voss, S.E., Rosowski, J.J., Merchant, S.N., Peake, W.T., 2000. Acoustic responses of the human middle ear. Hearing Research 150, 43–69.

Willi, U.B., Ferrazzini, M.A., Huber, A.M., 2002. The incudo-malleolar joint and sound transmission losses. Hearing Research 174, 32 – 44.

ACCEPTED MANUSCRIPT

Research highlights - “Biomechanics of the Incudo-Malleolar-Joint – Experimental Investigations for quasi-static loads”

Spatial displacements of isolated Malleus-Incus-Complex (MIC) for quasi-static loads were measured.

- Excitation at several points of the incus with a stylus connected to a load cell.
- Measurement Signals: Force and displacement applied by the stylus and spatial displacement.
- Reconstruction of the MIC geometry from micro-CT scans and of the spatial motion from 3D-Laser-Doppler-Vibrometry measurements.
- The relative motion within the joint changes as the load is increased.
- The change is caused by contact of the articular surfaces as shown by proximity calculations.
- The IMJ is a mechanical filter decoupling large quasi-static-loads while transferring dynamic sound events. This is realized by a diathroidal joint encapsuled by highly viscoelastic ligaments.

ACCEPTED MANUSCRIPT